

A PRINTED 2.4 GHz/5.8 GHz DUAL-BAND MONOPOLE ANTENNA WITH A PROTRUDING STUB IN THE GROUND PLANE FOR WLAN AND RFID APPLICATIONS

J. R. Panda and R. S. Kshetrimayum*

Department of Electronics and Electrical Engineering, Indian Institute of Technology, Guwahati 781039, India

Abstract—The design of a simple microstrip fed folded strip monopole antenna (FSMA) with a protruding stub in the ground plane for the application in WLAN and RFID is presented. The antenna has two resonant paths, one in the radiating element (folded strip) and the other in the protruding stub of the ground plane. It supports two resonances at 2.4 GHz and 5.81 GHz, which are the center frequencies of WLAN and RFID. Effectively consistent radiation pattern and large percentage bandwidth have been observed. The measured percentage fractional bandwidth at 2.4 GHz (2.05 GHz to 2.86 GHz) is 32.99, and the percentage fractional bandwidth at 5.81 GHz (5.55 GHz to 6.14 GHz) is 10.11. The proposed antenna is simple and compact in size, providing broadband impedance matching, consistent radiation pattern and appropriate gain characteristics in the WLAN and RFID frequency regions.

1. INTRODUCTION

Compact printed monopole antennas are indispensable for the application in wireless local area network (WLAN), ultra-wideband (UWB) and radio-frequency identification (RFID) applications. Along with the compact size, the antenna should be low cost, light weight, less fragile, low profile, and finally, the fabrication methodology should be simple. Many compact printed monopole antennas were fabricated for wireless applications and reported in the literature [1–7]. Most of these antennas are designed for applications either in WLAN [1–5]

Received 13 May 2011, Accepted 9 June 2011, Scheduled 16 June 2011

* Corresponding author: Rakesh Singh Kshetrimayum (rakesh@iieee.org).

2. ANTENNA DESIGN

The dual-band monopole antenna (DBMA) with a microstrip fed folded strip and a protruding stub in the ground plane is printed on the FR4 substrate of relative permittivity 4.4 and thickness 1.6 mm as shown in the Figure 1. A 50-Ohm microstrip line is used for the excitation. The folded strip width and protruding stub width of the proposed DBMA is 3 mm, same as that of the width of the microstrip line. The remaining design parameters are given in Figure 1.

Two resonance paths are clearly visible in the proposed antenna, one in the folded strip (L_α) of the radiating element and the other ($L_\beta = N$) in the protruding stub of the ground plane. The length of the resonant path in the folded strip is $L_\alpha = 29.8$ mm, which is $0.23\lambda_1$ at the first resonant frequency of 2.4 GHz ($f_1 = 2.4$ GHz). Similarly, the length of the second resonant path in the protruding stub of the ground plane is $L_\beta = N = 12$ mm, which is $0.23\lambda_2$ at the second resonance frequency of 5.8 GHz ($f_2 = 5.8$ GHz). By properly varying the lengths L_α and L_β , we can fix the antenna resonance at 2.4 GHz and 5.8 GHz, respectively. The overall adjustments of the geometrical parameters are done for the improvement of impedance bandwidth in the 2.4 GHz and 5.8 GHz bands. The full wave simulator IE3D [17] is used to simulate the proposed antenna.

3. RESULTS AND DISCUSSION

Figure 2 shows the photograph of the fabricated prototype of the proposed antenna for 2.4 GHz and 5.81 GHz for WLAN and RFID applications. Figure 3 shows the comparison of the simulated

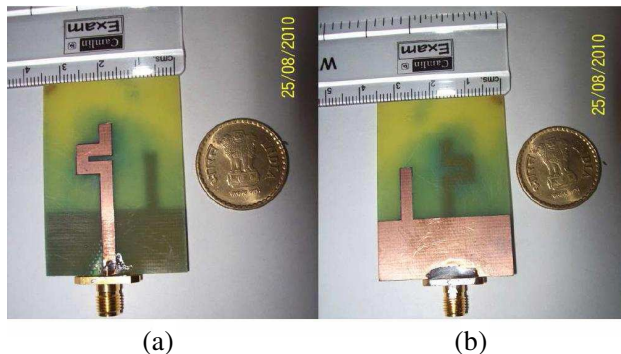


Figure 2. Fabricated folded strip monopole antenna with a protruding stub prototype. (a) Top view, (b) bottom view.

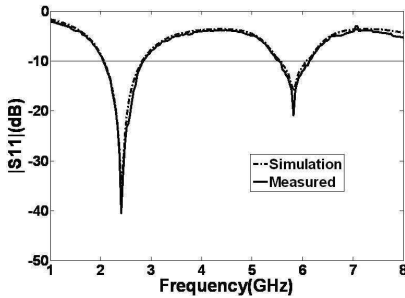


Figure 3. Comparison of the simulated and the measured reflection coefficients ($|S_{11}|$) (dB) of the proposed DBMA for WLAN and RFID applications.

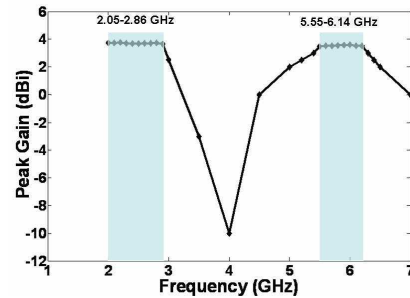


Figure 4. Measured peak gain (dBi) vs. frequency of the proposed antenna.

and measured graphs of the reflection coefficient ($|S_{11}|$) (dB) of the proposed antenna. The reflection coefficient measurement was performed by using Rohde and Schwarz ZVA24 vector network analyzer. From the graph, it is quite clear that there is reasonably good agreement between the measured and simulated reflection coefficients ($|S_{11}|$) (dB). The experimental versus simulated lower and upper cutoff frequencies present quite clearly a match and confirm good fabrication quality of the fabricated prototype. With the measurement, the first resonance occurs at 2.4 GHz having the reflection coefficient value of -40.48 dB with percentage fractional bandwidth (FBW) of 32.99 (2.05 GHz to 2.86 GHz), and the second resonance occurs at 5.81 GHz having the reflection coefficient value of -20.21 dB with percentage FBW of 10.11 (5.55 GHz to 6.14 GHz). Hence, from the experimental results, it is clear that the fabricated prototype can be used for the dual band WLAN and RFID applications around 2.4 GHz and 5.8 GHz.

Figure 4 shows the measured peak gain in dBi of the proposed antenna. The measured peak gain at 2.4 GHz is 3.7 dBi, and the measured peak gain at 5.8 GHz is 3.57 dBi. The measured peak gain is almost consistent in the frequency range of 2.05 GHz to 2.86 GHz, and the average peak gain in this frequency range is 3.73 dBi. Similar situation can be seen in the frequency range of 5.55 GHz to 6.14 GHz. The average measured peak gain in this frequency range is approximately 3.59 dBi.

Figure 5(a) shows the reflection coefficient for successive values of the distance M between the folded strip of the radiating element and the protruding stub in the ground plane when the other parameters such as N ($= 12$ mm) and P ($= 4.8$ mm) are kept constant. From the

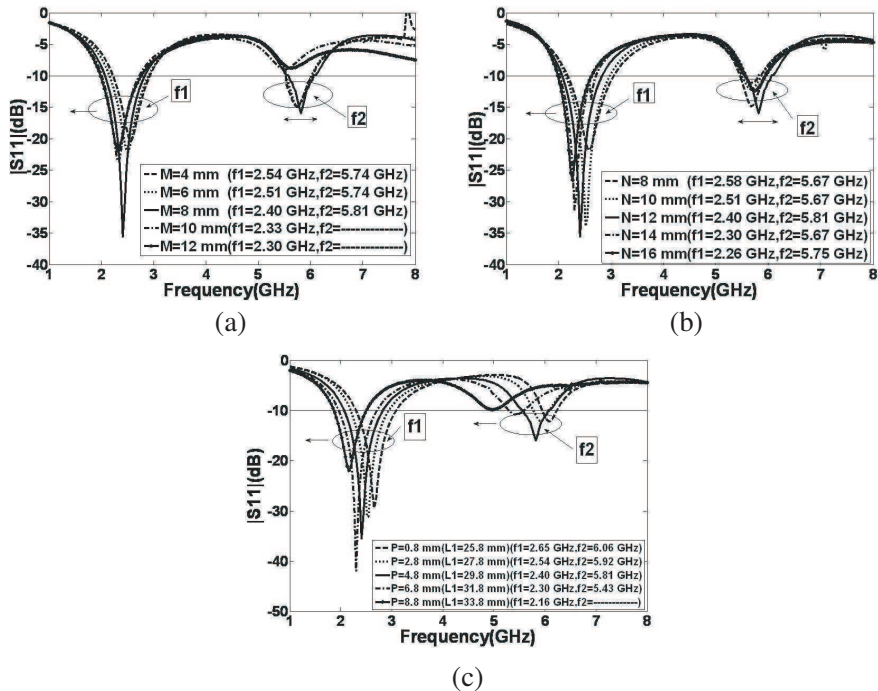


Figure 5. Simulated reflection coefficient ($|S_{11}|$) (dB) graphs, (a) M is a variable, $N = 12$ mm and $P = 4.8$ mm, (b) N is a variable, $M = 8$ mm and $P = 4.8$ mm, and (c) P is a variable, $M = 8$ mm and $N = 12$ mm.

graph, it is clearly visible that when M increases from 4 mm to 12 mm, the first resonant frequency (f_1) moves towards left, which means that the first resonant frequency (f_1) decreases with the increase of the distance M . On the other hand, the second resonant frequency (f_2) almost remains static at 5.8 GHz, but the performance degrades at $M = 10$ mm and 12 mm.

Figure 5(b) shows the reflection coefficient for successive values of the length N of the protruding stub in the ground plane when the other parameters such as M ($= 8$ mm) and P ($= 4.8$ mm) remain constant. From the graph, it can be seen that when N increases from 8 mm to 16 mm, the first resonant frequency (f_1) moves towards left, which means that the first resonant frequency (f_1) decreases rapidly with the increase of the length of the protruding stub N . On the other hand, very little shifting of second resonant frequency (f_2) occurs, which is less than the shifting of the first resonant frequency (f_1). Hence the

second resonant frequency (f_2) is almost independent of the variation of N , the length of the protruding stub.

Figure 5(c) shows the reflection coefficient for successive values of the length P of the radiating element (means also the total length of the folded strip ($L_1 = L_\alpha$)) when the other parameters such as M ($= 8\text{ mm}$) and N ($= 12\text{ mm}$) remain constant. From the graph, one can experience that when P increases from 0.8 mm to 8.8 mm , the first resonant frequency (f_1) moves towards left, which means that the first resonance frequency (f_1) decreases with the increase of the length P . On the other hand, the second resonant frequency (f_2) is also decreased with the increase of P , which means that the second resonant frequency (f_2) moves towards left, but the performance degrades at $P = 8.8\text{ mm}$. When the width of the folded portion of the radiating is varied, the first and second resonant frequencies increase with the increase of the width of the folded strip. In other words, both the resonant frequencies have shifted towards right when the width of the folded part of the radiating strip is increased. But at the higher width of the folded part of the radiating strip, the performance degrades for the second resonance frequency.

Figure 6 shows the measured normalized co- and cross-polar E -plane (xz -plane) radiation pattern of the proposed antenna at 2.4 and 5.8 GHz , respectively, and Figure 7 shows measured normalized co- and cross-polar H -plane (yz -plane) radiation pattern at 2.4 and 5.8 GHz , respectively. The co-polar H -plane radiation pattern is purely omnidirectional at all the measured frequencies. At 2.4 GHz , the cross-

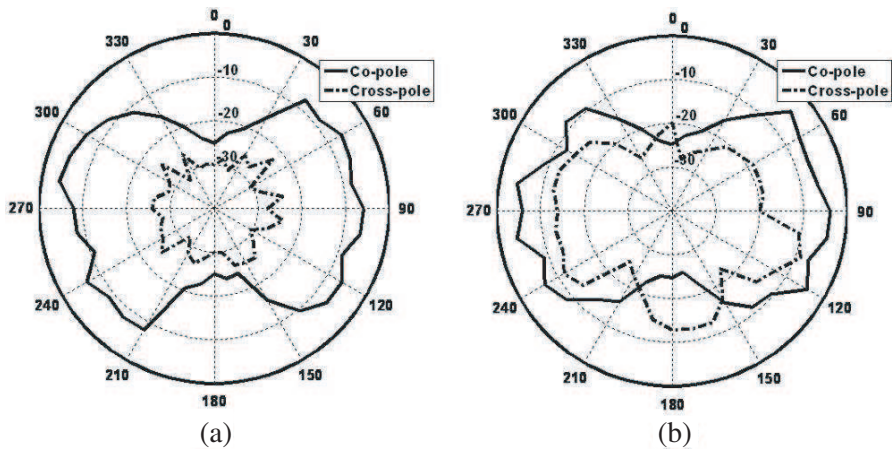


Figure 6. Measured E -plane (xz -plane) radiation patterns of the proposed antenna at (a) 2.4 GHz and (b) 5.8 GHz .

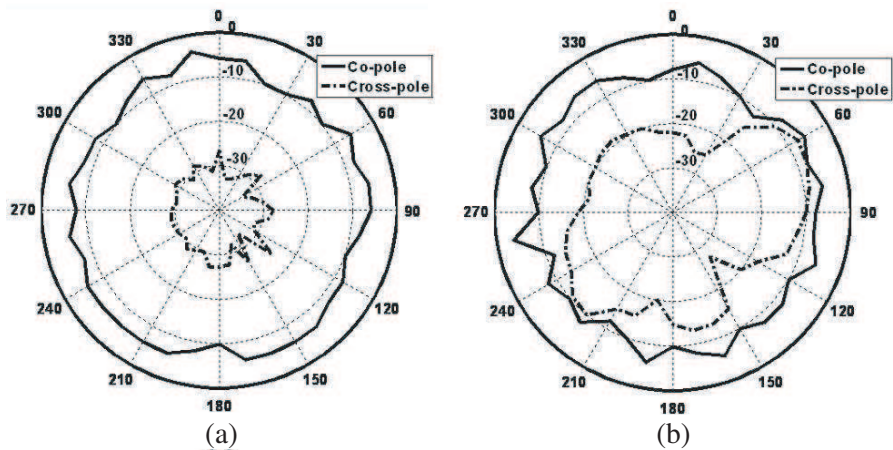


Figure 7. Measured H -plane (yz -plane) radiation patterns of the proposed antenna at (a) 2.4 GHz and (b) 5.8 GHz.

polar H -plane radiation is just around -30 dB and at 5.8 GHz, and the cross-polar H -plane radiation is in between -10 dB to -20 dB. The co-polar E -plane radiation pattern is directional along 90° and 270° , respectively. In the co-polar E -plane, the radiation patterns remain roughly dumbbell shaped like that of a small dipole which has bidirectional patterns. The cross-polar E -plane radiation is just around -30 dB, and at 5.8 GHz, the cross-polar E -plane radiation is in between -10 dB and -20 dB.

Figure 8(a) shows the surface current density distribution in the feed-line, folded strip and the protruding stub in the ground plane of the proposed antenna at 2.4 GHz. The directions of currents in the feed-line and ground plane are opposite in nature. It can be observed that strong surface current flows from the top to bottom (downward direction) of the folded strip of length (L_α). Due to this heavy flow of surface current in the folded strip, strong resonance occurs at 2.4 GHz. Whereas in the protruding stub (L_β) in the ground plane, a mild current is flowing in upward direction. This is the reason that the protruding stub in the ground plane does not produce a good resonance at 5.8 GHz.

Similarly at 5.8 GHz, the surface current distribution in the feed-line, folded strip and the protruding stub in the ground plane of the proposed antenna is depicted in Figure 8(b). At 5.8 GHz, the current densities at the feed-line and ground plane are opposite in direction. The direction of current in the folded strip (L_α) is from the bottom to top (upward direction). A strong current is also available in the

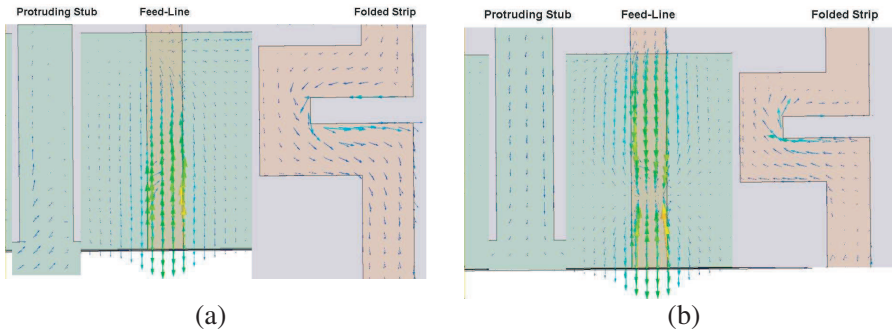


Figure 8. Surface current density of the ground plane of the proposed antenna at (a) 2.4 GHz and (b) 5.8 GHz.

folded strip at 5.8 GHz which gives strong resonance at 5.8 GHz. At the same time in the protruding stub (L_β) in the ground plane, a very weak current flows from top to bottom (downward direction). Hence, the protruding stub in the ground plane also does not produce a good resonance at 5.8 GHz.

Hence from the above discussion on the current distribution in the proposed antenna at 2.4 and 5.8 GHz, a conclusion has come out as that at 2.4 and 5.8 GHz, a strong current density is available in either direction in the folded strip. This is the reason that the antenna radiates strongly and simultaneously at 2.4 and 5.8 GHz as the current density is high in the folded strip at the two frequencies. But at the same time, in the protruding stub of the ground plane, the current density has never built up for the antenna to strongly radiate at 2.4 GHz and 5.8 GHz. The electromagnetic coupling effect has also controlled the two excited resonant frequencies at 2.4 GHz and 5.8 GHz between the folded strips (L_α) and the protruding stub (L_β) in the ground plane.

4. CONCLUSION

A simple microstrip fed folded strip monopole antenna with a protruding stub in the ground plane for application in WLAN and RFID is designed. Satisfactory dual-band operation for WLAN and RFID application can be easily achieved by the proposed antenna, which provides two resonant paths of different lengths for the excitation of the two resonant frequencies. The proposed antenna is simple and compact in size, providing broadband impedance matching, consistent radiation pattern and appropriate gain characteristics in the WLAN and RFID frequency ranges. Hence the proposed antenna may be a

suitable candidate for the dual-band operation in WLAN and RFID applications.

ACKNOWLEDGMENT

The authors would like to thank U. K. Sarma and D. Goswami of IIT Guwahati, G. Hemanth and Hemalatha of IISc Bangalore for their assistance in fabrication and measurement of the proposed antennas. The second author is grateful to Dr. K. J. Vinoy of IISc Bangalore and Prof. A. Mahanta of IIT Guwahati for allowing the first author to use their laboratories for various measurements of the proposed antenna.

REFERENCES

1. Shams, K. M. Z., M. Ali, and H.-S. Hwang, "A planar inductively coupled bow-tie slot antenna for WLAN application," *Journal of Electromagnetic Waves and Applications*, Vol. 20, No. 7, 861–871, 2006.
2. Zhang, T.-L., Z.-H. Yan, L. Chen, and Y. Song, "A compact dual-band CPW-fed planar monopole antenna for WLAN applications," *Journal of Electromagnetic Waves and Applications*, Vol. 22, Nos. 14–15, 2097–2104, 2008.
3. Jaw, J.-L., F.-S. Chen, and D.-F. Chen, "Compact dualband CPW-fed slotted patch antenna for 2.4/5 GHz WLAN operation," *Journal of Electromagnetic Waves and Applications*, Vol. 23, Nos. 14–15, 1947–1955, 2009.
4. Liu, W.-C., P.-W. Chen, and C.-C. Liu, "Triple-band planar monopole antenna for DMB/WLAN applications," *Journal of Electromagnetic Waves and Applications*, Vol. 24, Nos. 5–6, 653–661, 2010.
5. Zhao, K., S. Zhang, and S. L. He, "Closely-located MIMO antennas of tri-band for WLAN mobile terminal applications," *Journal of Electromagnetic Waves and Applications*, Vol. 24, Nos. 2–3, 363–371, 2010.
6. Chen, W. S. and Y.-H. Yu, "Dual-band printed dipole antenna with parasitic element for WIMAX applications," *IEE Electronics Letters*, Vol. 44, No. 23, 1338–1339, Nov. 2008.
7. Chang, T.-N., G.-Y. Shen, and J.-M. Lin, "CPW-fed antenna covering WiMAX 2.5/3.5/5.7 GHz bands," *Journal of Electromagnetic Waves and Applications*, Vol. 24, Nos. 2–3, 189–197, 2010.
8. Kuo, Y.-L. and K. L. Wong, "Printed double-T monopole antenna

- for 2.4/5.2 GHz dual-band WLAN operation,” *IEEE Transactions on Antennas and Propagation*, Vol. 51, No. 9, 2187–2191, 2003.
9. Liu, W.-C., W. R. Chen, and C. M. Wu, “Printed double S-shaped monopole antenna for wideband and multiband operation of wireless communication,” *IEE Proceedings Microwaves, Antennas and Propagation*, Vol. 151, No. 6, 473–476, 2004.
 10. Liu, W.-C., “Optimal design of dualband CPW-fed G-shaped monopole antenna for WLAN application,” *Progress In Electromagnetics Research*, Vol. 74, 21–38, 2007.
 11. Liu, Z.-Y., Y.-Z. Yin, L.-H. Wen, W.-C. Xiao, Y. Wang, and S.-L. Zuo, “A Y-shaped tri-band monopole antenna with a parasitic M-strip for PCS and WLAN applications,” *Journal of Electromagnetic Waves and Applications*, Vol. 24, Nos. 8–9, 1219–1227, 2010.
 12. Liu, W. C. and C.-F. Hsu, “Dual-band CPW-fed Y-shaped monopole antenna for PCS/WLAN application,” *IEE Electronics Letters*, Vol. 41, No. 7, 390–391, 2005.
 13. Wu, C.-M., “Dual-band CPW-fed cross-slot monopole antenna for WLAN operation,” *IET Microwaves, Antennas and Propagation*, Vol. 1, No. 2, 542–546, 2007.
 14. Bao, X. L. and M. J. Ammann, “Microstrip-fed dual-frequency annular-slot antenna loaded by split-ring-slot,” *IET Microwaves, Antennas and Propagation*, Vol. 3, No. 5, 757–764, 2009.
 15. Liu, W.-C., C.-M. Wu, and N.-C. Chu, “A compact CPW-fed slotted patch antenna for dual-band operation,” *IEEE Antennas and Wireless Propagation Letters*, Vol. 9, 110–113, 2010.
 16. Hsieh, C., T. Chiu, and C. Lai, “Compact dual-band slot antenna at the corner of the ground plane,” *IEEE Transactions on Antennas and Propagation*, Vol. 57, No. 10, 3423–3426, 2009.
 17. IE3D version 10.2, Zeland Corp, Fremont, CA, USA.